Varying Constants and Fundamental Cosmology ,
12-17 Sep 2016, Szczecin, Poland

The false vacuum bubble as the creation of our universe

Wonwoo Lee
(Center for Quantum Spacetime, Sogang University)

based on
Bum-Hoon Lee, Chul H. Lee, WL, Changheon Oh
CQG26, 225002 (2009), PRD82, 024019 (2010), & IJMPA30, 1550110 (2015)

The plan of this talk

1. Motivation
2. Tunneling of a particle through a potential barrier:
   WKB approximation
3. The first order phase transition of a scalar field:
   Nucleation of vacuum bubbles
4. Effects of the self gravity on the bubble nucleation
5. Classification of true vacuum bubbles
6. Tunneling instanton solutions
7. The creation of our universe (From zero to eternity) :
   The nucleation of false vacuum bubbles
8. Summary and discussions

1. MOTIVATIONS

(1) Classification of vacuum bubbles

(2) Study on the non-perturbative self-gravitating solutions

(3) Dynamical change of the cosmological constant

(4) Modification of the concept of the terminal vacuum or sink in the cosmic landscape

Bousso and Polchinski, JHEP. 06, 006 (2000), Susskind, arXiv:hep-th/0302219.

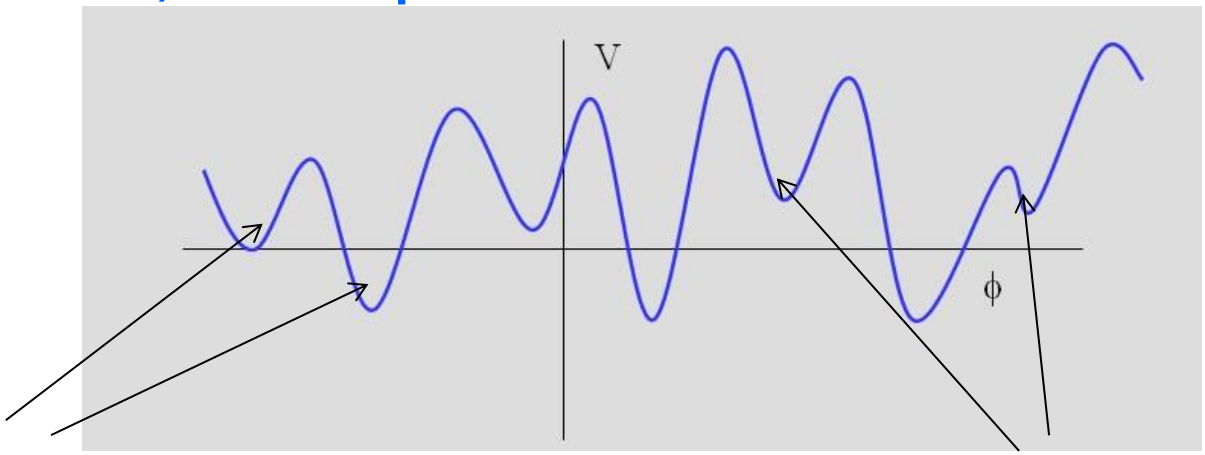

terminal vacuum or sink

recyclable or transient

(5) Can we understand how our universe was created or began?

What is origin of our universe?

Nothing? (past finite time)

Something? (past infinite time)

The scenario of a self-creating universe?
(CTC or past infinite time)

Inflationary universe scenario

Solves horizon problem, flatness problem, …

Early universe with the low entropy

the entropy was generated by the reheating process

Conceptual problem :
incompleteness in the past direction
-> initial singularity persists

That is to say, the inflationary cosmology must be incomplete in the past direction.

“Borde, Guth, and Vilenkin, PRL, 90, 151301 (2003)”

(6) Inflationary multiverse scenario or Eternal universe

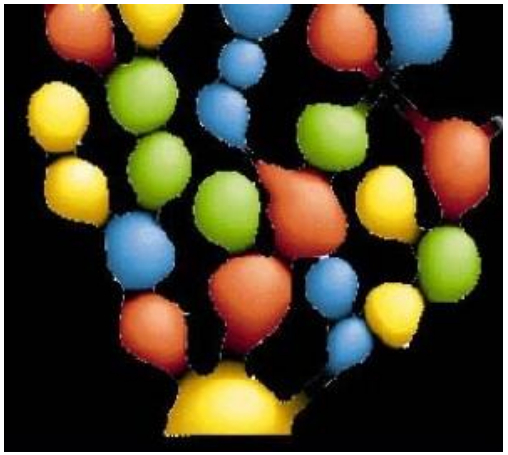

Linde, Vilenkin, Guth

A. Linde (1982) wanted to suggest a universe without the cosmological singularity problem using an interesting feature of self-reproducting or regenerating exponential expansion of the universe.

Future eternal, not past eternal!
by BGV (2003)

The universe as a whole does not have a single beginning.

Quantum cosmology (DeWitt, PR160, 1113 (1967), Hartle & Hawking, PRD28, 2960 (1983), Vilenkin, PRD30, 509 (1984))

before → after

nothing ⇒ Something, homogeneous

to avoid the singularity problem of a Universe

the no-boundary proposal of the Wheeler-DeWitt equation by Hartle and Hawking

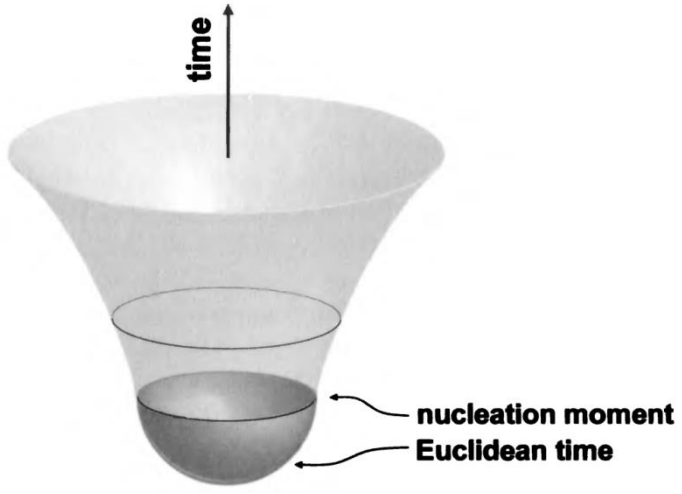

Nothing would be unstable!

(7) Why the universe begun with the very low entropy?

Boltzmann, Tolman, Penrose, Carroll, …

(8) Making the de Sitter spacetime even in flat or AdS spacetime

(i) nucleation of a de Sitter bubble

(ii) topological inflation as an instanton solution

(iii) an instanton-induced domain wall or braneworld rather than a kink-induced domain wall

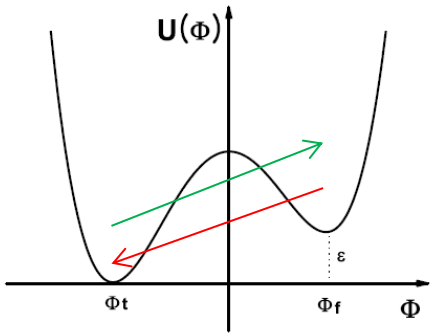

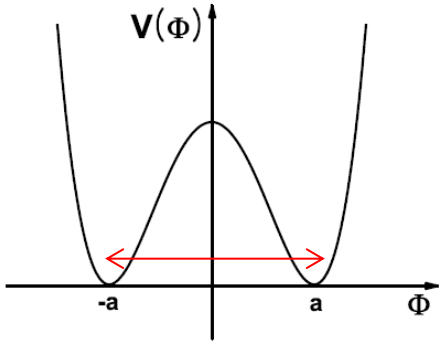

- **The tunneling process becomes a remarkable event in these frameworks.**

- **We try to understand the creation of our universe with the mechanism of the nucleation of a vacuum bubble or a domain wall or inflating region.**

- **The important thing is the fact that, once the de Sitter vacuum can exist, the inflationary expansion is eternal into the future and has the possibility of self-reproduction.**

2. Tunneling of a particle through a potential barrier: WKB approximation

A particle of unit mass moving in 1-dimensional space

$$L = \frac{1}{2}\left(\frac{dq}{dt}\right)^2 - V(q)$$

Quantum mechanically, the particle originally located at q_o can penetrate the potential barrier and materialize at σ.

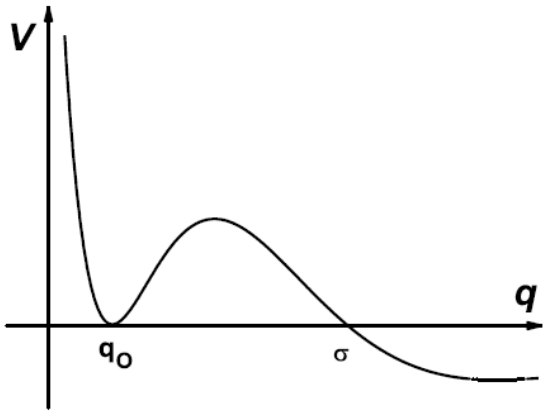

To calculate the probability for such tunneling using the WKB approximation, one considers the Euclidean action

$$I_E = \int_{-\infty}^{\infty} d\tau L_E, \quad L_E = \frac{1}{2}\left(\frac{dq}{d\tau}\right)^2 + V(q)$$

The corresponding Euclidean equation of motion

$$\frac{d^2q}{d\tau^2} = -\frac{\partial(-V)}{\partial q}$$

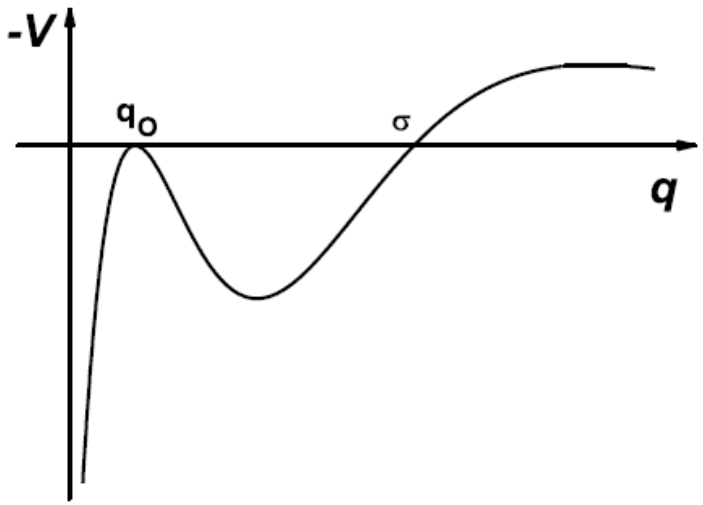

The solution satisfying the boundary condition

$$\lim_{\tau\to\pm\infty} q(\tau) = q_o, \quad \left.\frac{dq}{d\tau}\right|_{q=\sigma(\tau=0)} = 0$$

is called the bounce.

Then the probability is calculated, in the WKB approximation, by

$$\Gamma \sim Ae^{-B/\hbar}$$

where B is the Euclidean action of the bounce and A is the determinant factor from the quantum correction

3. The first order phase transition of a scalar field: nucleation of vacuum bubbles

The case of a scalar field with the potential having two minima, one corresponding to the false vacuum, the other to the true vacuum. (gravity ignored)

$$\mathcal{L} = -\frac{1}{2}\eta^{\mu\nu}\partial_\mu\Phi\partial_\nu\Phi - U(\Phi)$$

M.B. Voloshin, I. Yu. Kobzarev, & L.B. Okun,
Yad. Fiz. **20** (1974) [Sov. J. Nucl. Phys. **20** (1975)]
S. Coleman, PRD**15** (1977),
C. Callan Jr. & S. Coleman PRD**16** (1997)

The Euclidean action

$$I_E = \int d\tau d^3x \mathcal{L}_E = \int d\tau d^3x \left[\frac{1}{2}\left(\frac{d\Phi}{d\tau}\right)^2 + \frac{1}{2}|\nabla\Phi|^2 + U(\Phi)\right]$$

the corresponding Euclidean field equation

$$\frac{\partial^2\Phi}{\partial\tau^2} + \nabla^2\Phi = \frac{\partial U}{\partial\Phi}$$

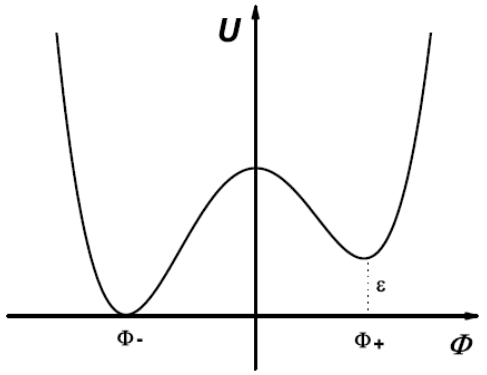

$$U(\Phi) = \frac{\lambda}{8}\left(\Phi^2 - \frac{\mu^2}{\lambda}\right)^2 - \frac{\epsilon\sqrt{\lambda}}{2\mu}\left(\Phi - \frac{\mu}{\sqrt{\lambda}}\right) + U_o$$

A bounce is a solution of the Euclidean field equation satisfying appropriate boundary conditions.

The nucleation rate of a true vacuum bubble in the sea of the false vacuum background is obtained by

$$\Gamma \sim Ae^{-B/\hbar}$$

where B is the Euclidean action of the bounce

$$B = \int d\tau d^3x \mathcal{L}_E^{(b)}$$

If there are several bounces the main contribution comes from the one with the least Euclidean action.

The bounce with the least Euclidean action is assumed to have the highest symmetry, and the solution with O(4) symmetry is considered. Then Φ depends only on $\eta(=\sqrt{\tau^2+|x|^2})$, and the Euclidean field equation becomes

$$\frac{d^2\Phi}{d\eta^2} + \frac{3}{\eta}\frac{d\Phi}{d\eta} = -\frac{d(-U)}{d\Phi}$$

It can be treated like a one-particle equation of motion with playing the role of time. The boundary conditions for the bounce are

$$\Phi(\eta)|_{\eta=\infty} = \Phi_+ \quad \text{and} \quad \frac{d\Phi}{d\eta}|_{\eta=0} = 0$$

Multiplying the field equation with $d\Phi/d\eta$ **One obtains**

$$\frac{d}{d\eta}\left[\frac{1}{2}\left(\frac{d\Phi}{d\eta}\right)^2 - U\right] = -\frac{3}{\eta}\left(\frac{d\Phi}{d\eta}\right)^2$$

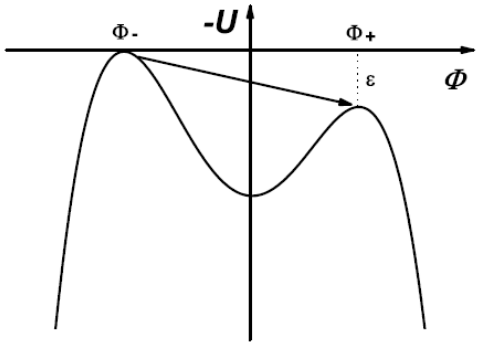

The quantity in the square parentheses can be interpreted as the total energy of the particle with the potential energy –U, the term on the right hand side as the dissipation rate of the total energy.

-U at the starting point has to be higher than that at Φ_+ **.;**
Nucleation of a false vacuum bubble in the true vacuum background is not possible.

The general feature of the solution, particularly in the thin wall approximation, looks like the diagram

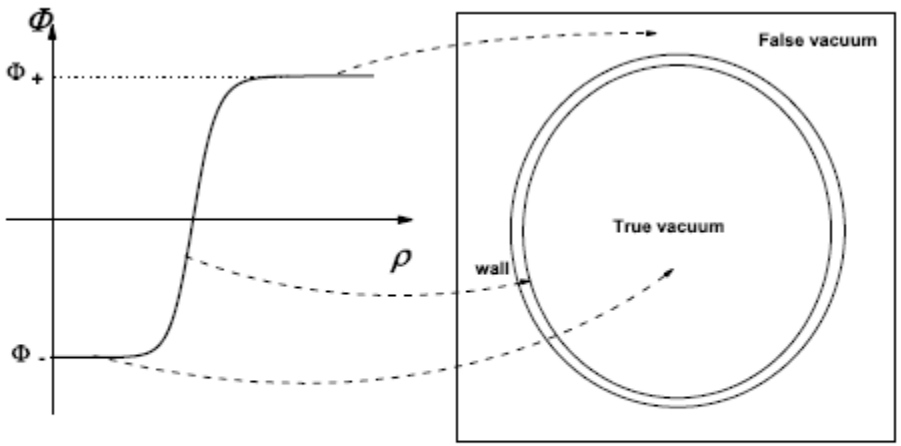

Typical vacuum bubble profile with the transitional region (wall) in the middle.

Dynamics of a nucleated vacuum bubble

The flat space the metric with *O*(4) symmetry

$$ds^2 = d\eta^2 + \eta^2[d\chi^2 + \sin^2\chi(d\theta^2 + \sin^2\theta d\phi^2)]$$

Lorentzian solutions by applying the analytic continuation

$$\chi \to i\chi + \frac{\pi}{2}$$

Then the metric

$$ds^2 = d\eta^2 + \eta^2[-d\chi^2 + \cosh^2\chi(d\theta^2 + \sin^2\theta d\phi^2)]$$

By the coordinate transformation

$$r = \eta \cosh \chi \quad \text{and} \quad t = \eta \sinh \chi$$

then

$$ds^2 = -dt^2 + dr^2 + r^2 d\theta^2 + r^2 \sin^2 \theta d\phi^2$$

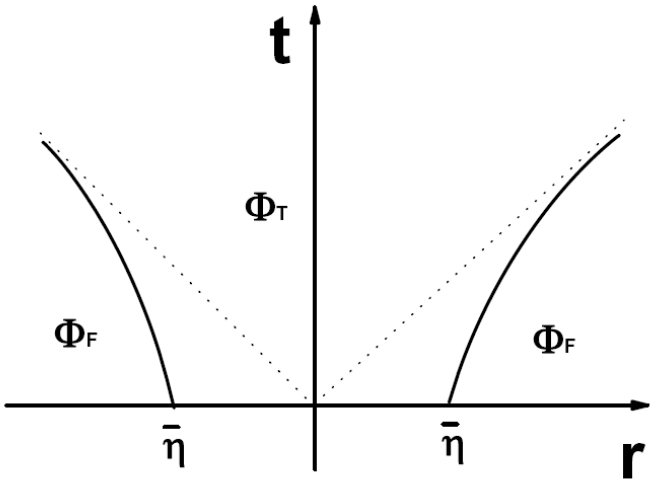

$$v = \frac{t}{\sqrt{t^2 + \bar{\eta}^2}}$$

$$a = \frac{1}{t}\left[\frac{1}{(1+\frac{\bar{\eta}^2}{t^2})^{1/2}} - \frac{1}{(1+\frac{\bar{\eta}^2}{t^2})^{3/2}}\right]$$

The figure represents the growth of a vacuum bubble after its materialization.

4. Effect of the self gravity on bubble nucleation

The case of a scalar field with its self-gravity fully considered (minimal coupling).

S. Coleman & F. De Luccia, PRD**21** (1980)

The total Lagrangian density of the system contains the matter part and the gravity part

$$\mathcal{L} = \mathcal{L}^{(M)} + \mathcal{L}^{(G)}$$

$$\mathcal{L}^{(M)} = -\frac{1}{2} g^{\mu\nu} \partial_\mu \Phi \partial_\nu \Phi - U(\Phi), \quad \mathcal{L}^{(G)} = -\frac{1}{16\pi G} R.$$

To search for the bounce with the minimum Euclidean action, O(4) symmetry is assumed for both Φ and the metric $g_{\mu\nu}$. The metric can be written in the form

$$ds^2 = d\eta^2 + \rho^2(\eta)[d\chi^2 + \sin^2\chi(d\theta^2 + \sin^2\theta d\phi^2)]$$

The Euclidean Lagrangian density becomes

$$\mathcal{L}_E = \frac{1}{2}\Phi'^2 + U + \frac{3}{8\pi G}\left(\frac{\rho''}{\rho} + \frac{\rho'^2}{\rho^2} - \frac{1}{\rho}\right)$$

where Φ and $g_{\mu\nu}$ are functions of η only and ‘ denotes the differentiation with respect to η .

The Euclidean field equations for Φ and ρ turn out to be

$$\Phi'' + \frac{3\rho'}{\rho}\Phi' = \frac{dU}{d\Phi}$$

$$\rho'' = -\frac{\kappa}{3}\rho(\Phi'^2 + U)$$

$$\rho'^2 - 1 - \frac{\kappa\rho^2}{3}\left(\frac{1}{2}\Phi'^2 - U\right) = 0$$

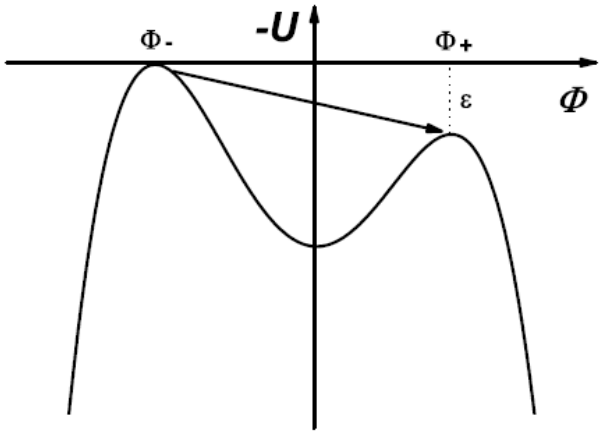

which can again be interpreted as a one-particle equation of motion with the second term being the dissipation term.

Typical solutions with the boundary conditions

$$\Phi(\eta)|_{\eta=\eta_{max}} \simeq \Phi_+ \quad \text{and} \quad \left.\frac{d\Phi}{d\eta}\right|_{\eta=0} = 0 \qquad \rho|_{\eta=0} = 0, \qquad \left.\frac{d\rho}{d\eta}\right|_{\eta=0} = 1,$$

The solutions are

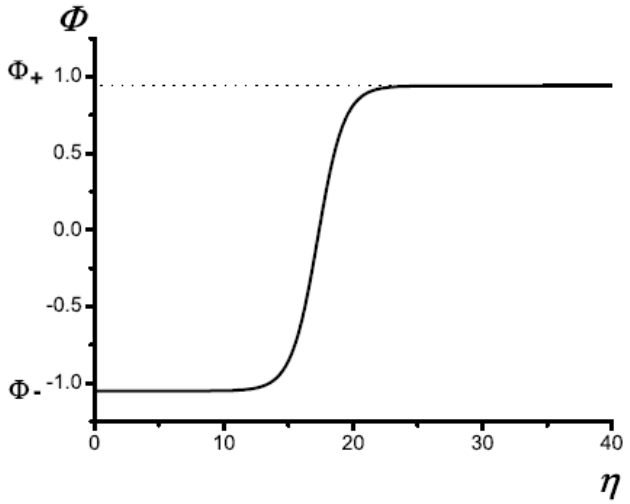

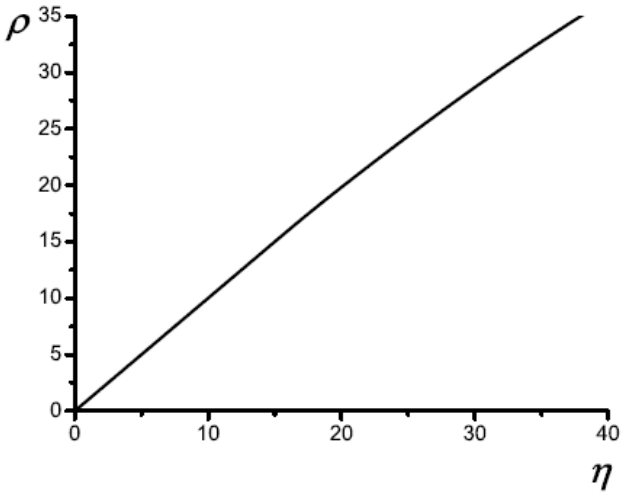

5. Classification of true vacuum bubbles

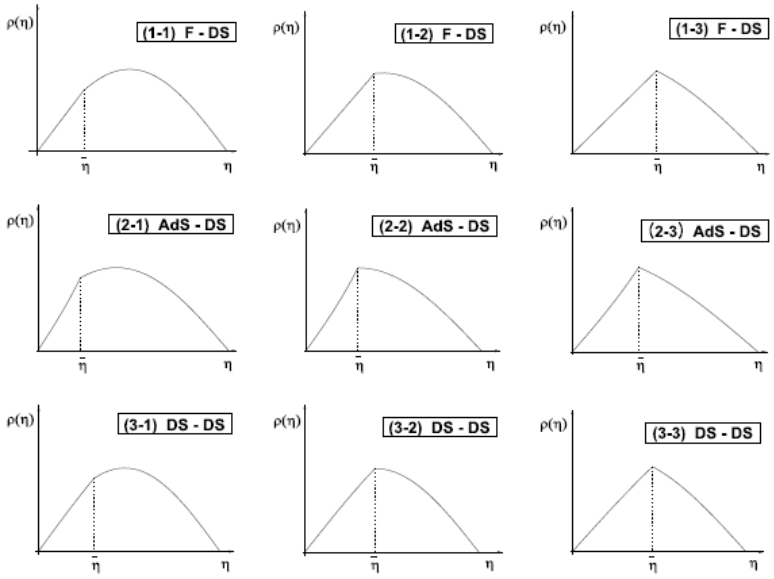

Figure 1-A

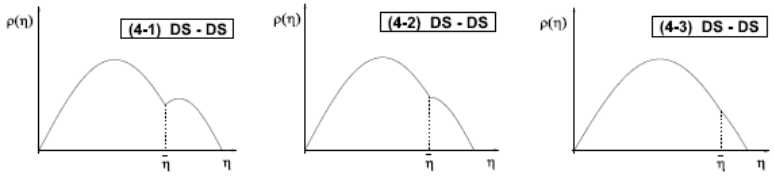

Figure 1-B

Figure 1: The schematic diagram for 12 possible types of true vacuum bubbles or matching with the thin-wall approximation. The $\bar{\eta}$ indicates the location of the wall. All the nine cases in Figure 1-A are possible solutions. The cases (4-1) - (4-3) in Figure 1-B don't have the stationary point in the action, allowing no solutions.

B.-H. Lee & WL, CQG 26, 225002 (2009)

We consider possible types of true vacuum bubbles. The exterior geometry of the bubble will remain to be de Sitter (dS) space. The true vacuum bubble can be classified according to the interior geometry and the size of the bubble. The schematic diagrams of twelve possible types of solutions with different shapes are illustrated in Fig.1.

When the geometry of the bubble (or background space) is de Sitter, the size of the bubble (or background space) will be called "small" or "large" depending on whether its size is smaller than or larger than half of the de Sitter space itself.

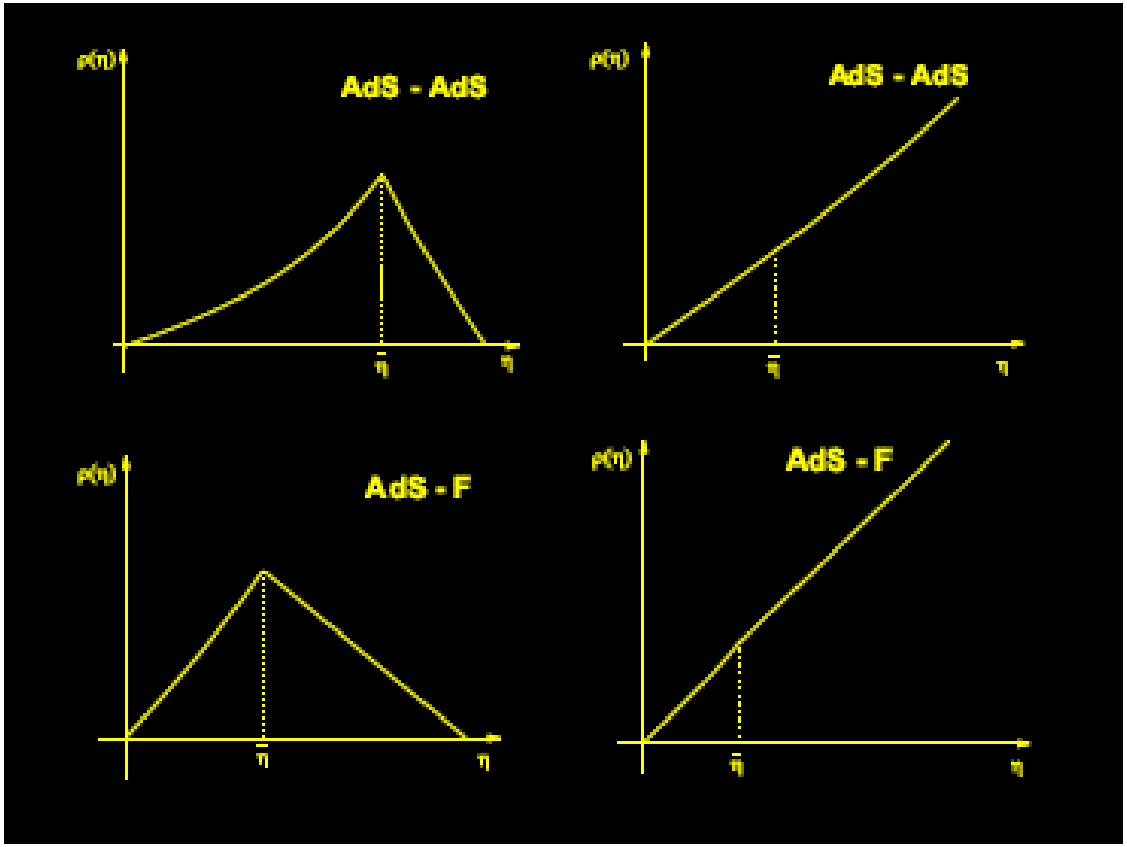
ρ(η)
AdS - AdS
η̄
η
ρ(η)
AdS - AdS
η̄
η
ρ(η)
AdS - F
η̄
η
ρ(η)
AdS - F
η̄
η

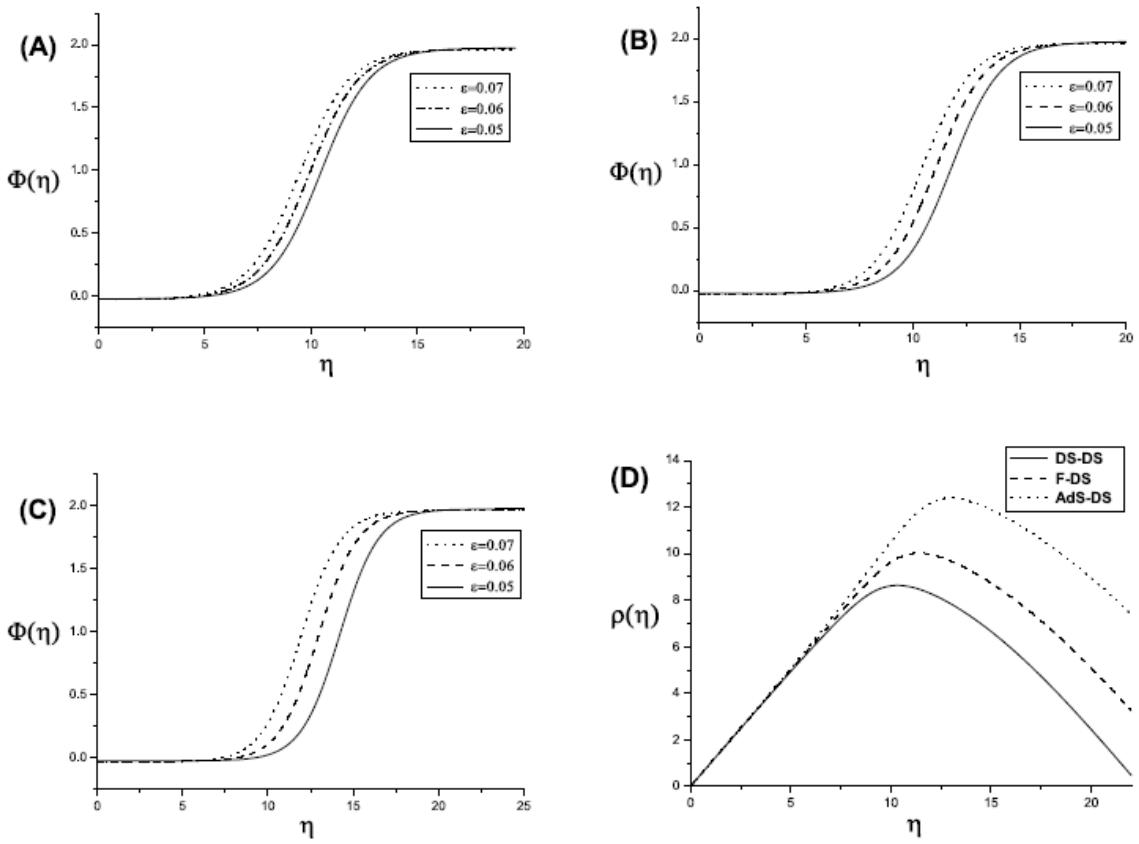

Figure 2: Numerical solutions for several types of true vacuum bubbles. We take $\tilde{\kappa} \simeq 0.3849$ for all cases. The first three figures are: (A) large flat bubble - small dS background corresponding to (1-3) in Fig. 1; (B) large AdS bubble - small dS background corresponding to (2-3); (C) large dS bubble - small dS background corresponding to (3-3). In Fig. (D), we take $\tilde{\epsilon} = 0.07$. We can see from these figures that the radius of a bubble becomes larger as $\tilde{\epsilon}$ becomes smaller.

6. Tunneling instanton solutions

B.-H. Lee, C. H. Lee, WL, & C. Oh,
PRD82, 024019 (2010)

Let us consider the action:

$$S = \int_{\mathcal{M}} \sqrt{-g} d^4x \left[\frac{R}{2\kappa} - \frac{1}{2} \nabla^\alpha \Phi \nabla_\alpha \Phi - U(\Phi) \right] + \oint_{\partial \mathcal{M}} \sqrt{-h} d^3x \frac{K - K_o}{\kappa},$$

the potential has the degenerate vacua

$$U(\Phi) = \frac{\lambda}{8} \left(\Phi^2 - \frac{\mu^2}{\lambda} \right)^2 + U_0$$

It is possible that the tunneling occurs via the potential with degenerate vacua in de Sitter space. The numerical solution Φ of this tunneling in fixed dS was obtained by Hackworth and Weinberg.

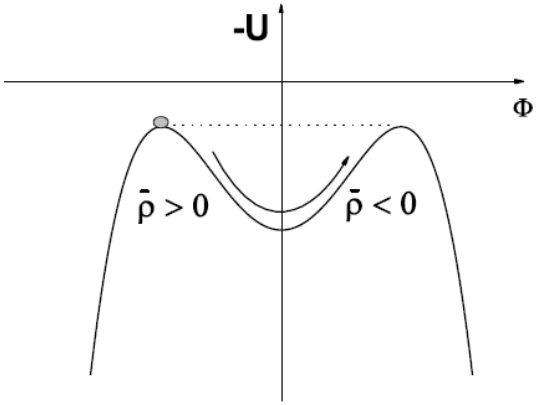

This tunneling is possible due to the changing role of the second term in Euclidean equation from damping to accelerating during the phase transition.

$$\Phi'' + \frac{3\rho'}{\rho}\Phi' = \frac{dU}{d\Phi}$$

Numerical solutions

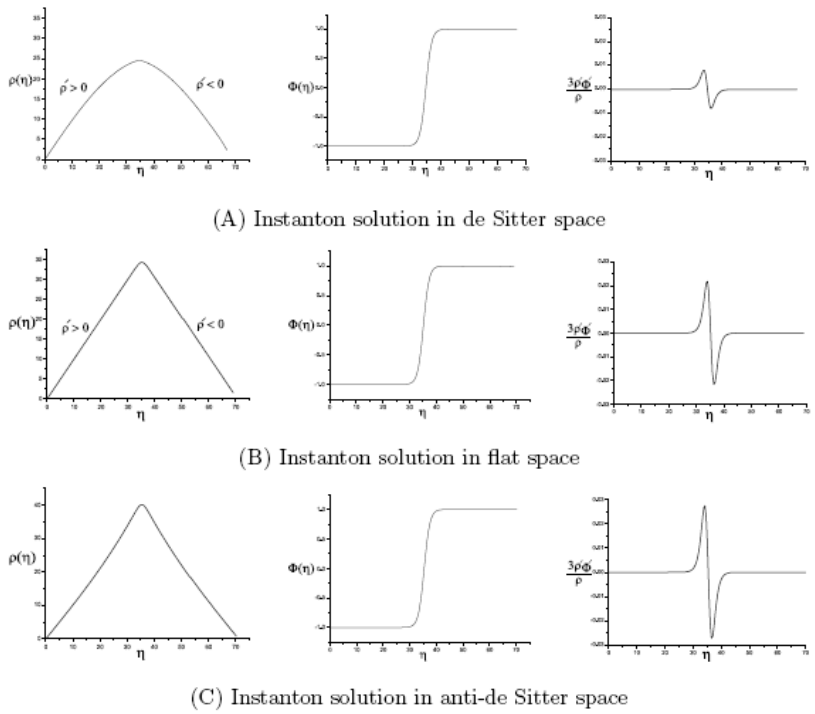

(A) Instanton solution in de Sitter space

(B) Instanton solution in flat space

(C) Instanton solution in anti-de Sitter space

Figure 1: The first and second columns show the numerical solutions on ρ and Φ, respectively. The third column shows the evolution of the second term in the left one of Eq. (4). The first row (A) illustrates the transition between the degenerate vacua in dS space, $\hat{U}_o = 0.01$ and $\hat{\kappa} \simeq 0.0474$. The second row (B) illustrates the transition between the degenerate vacua in flat space, $\hat{U}_o = 0$ and $\hat{\kappa} \simeq 0.1805$. The third row (C) illustrates the transition between the degenerate vacua in AdS space, $\hat{U}_o = -0.01$ and $\hat{\kappa} \simeq 0.2392$.

B.-H. Lee, C. H. Lee, WL, & C. Oh, PRD82, 024019 (2010)

The condition for the change of sign depends on the maximum value of the potential. To allow the change during the transition, the local maximum value of the potential U_{top} must be positive.

$$U(0) = \frac{3}{\kappa\rho^2} + \frac{1}{2}\Phi'|^2_{(\Phi=0)} > 0.$$

In other words,

$$-\mu^4/8\lambda < U_o$$

Two observer's point of view

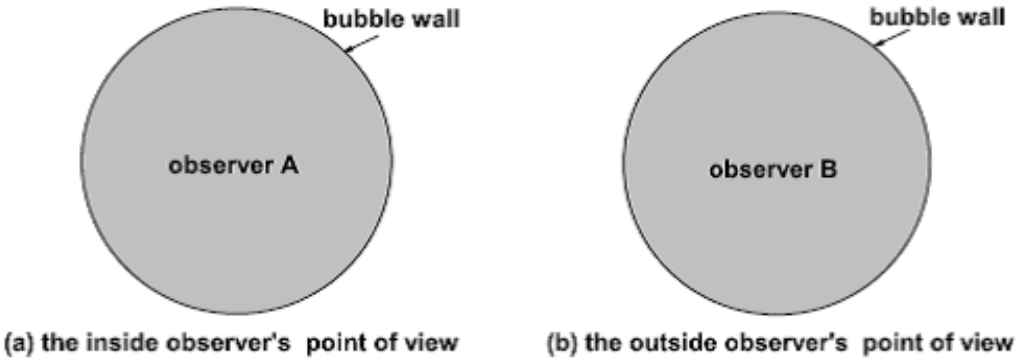

(a) the inside observer's point of view (b) the outside observer's point of view

We proposed the solutions with exact Z_2 symmetry can represent the nucleation of the braneworld-like object if the mechanism is applied in higher-dimensional theory. The braneworld having the finite size with the exact Z_2 symmetry can be nucleated not only in dS but also in flat and AdS bulk spacetime, and then expand, seen from an observer's point of view on the wall, without eating up bulk (inside and outside) spacetime.

Boundary conditions

B.-H. Lee, C. H. Lee, WL, & C. Oh, PRD85, 024022 (2012)

(i) Initial value problem

$$\rho|_{\eta=0} = 0, \quad \left.\frac{d\rho}{d\eta}\right|_{\eta=0} = 1, \quad \Phi|_{\eta=0} = \Phi_o, \quad \text{and} \quad \left.\frac{d\Phi}{d\eta}\right|_{\eta=0} = 0,$$

(ii) boundary value problem

$$\rho|_{\eta=0} = 0, \quad \rho|_{\eta=\eta_{max}} = 0, \quad \left.\frac{d\Phi}{d\eta}\right|_{\eta=0} = 0, \quad \text{and} \quad \left.\frac{d\Phi}{d\eta}\right|_{\eta=\eta_{max}} = 0.$$

For this procedure we choose the initial values of

$$\tilde{\Phi}(\tilde{\eta}_{initial}),\ \tilde{\Phi}'(\tilde{\eta}_{initial}),\ \tilde{\rho}(\tilde{\eta}_{initial}),\ \text{and}\ \tilde{\rho}'(\tilde{\eta}_{initial})\ \text{at}\ \tilde{\eta} = \tilde{\eta}_{initial}$$

$$\begin{aligned}
\tilde{\Phi}(\tilde{\eta}_{initial}) &\sim \tilde{\Phi}_0 + \frac{\epsilon^2}{16}\tilde{\Phi}_0\left(\tilde{\Phi}_0^2 - 1\right) + \frac{\epsilon^3}{48}\left(3\tilde{\Phi}_0^2 - 1\right), \\
\tilde{\Phi}'(\tilde{\eta}_{initial}) &\sim \frac{\epsilon}{8}\tilde{\Phi}_0\left(\tilde{\Phi}_0^2 - 1\right) + \frac{\epsilon^2}{16}\left(3\tilde{\Phi}_0^2 - 1\right), \\
\tilde{\rho}(\tilde{\eta}_{initial}) &\sim \epsilon, \\
\tilde{\rho}'(\tilde{\eta}_{initial}) &\sim 1,
\end{aligned}$$

Where $\tilde{\eta}_{initial} = 0 + \epsilon\ \text{and}\ \epsilon \ll 1$

If we find the initial value $\tilde{\Phi}_0$, other conditions are given by the above eqs. To avoid a singular solution at $\tilde{\eta} \to \tilde{\eta}_{max}$ and demand the Z_2 symmetry, the conditions $d\tilde{\Phi}/d\tilde{\eta} \to 0\ \text{and}\ \tilde{\rho} \to 0$ as $\tilde{\eta} \to \tilde{\eta}_{max}$ are needed. In this work we require that a value of $d\tilde{\Phi}/d\tilde{\eta}$ goes to the value smaller than 10^-6 as $\tilde{\eta} \to \tilde{\eta}_{max}$, because the exact value of $\tilde{\eta}_{max}$ is not known.

1.Oscillaing solutions between flat-flat degenerate vacua ($\tilde{\kappa} = 0.2$)

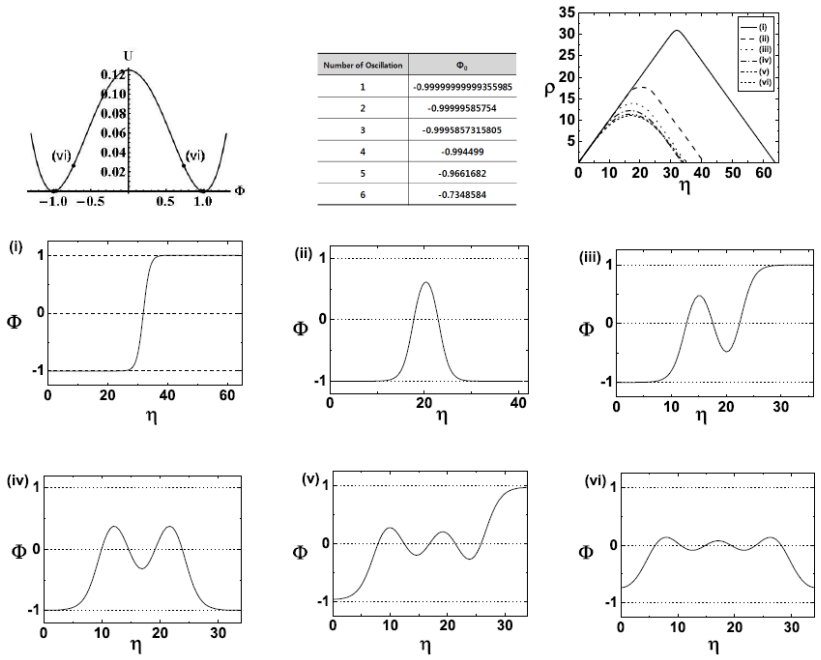

Number of Oscillation	Φ_0
1	-0.99999999999355985
2	-0.99999585754
3	-0.9995857315805
4	-0.994499
5	-0.9661682
6	-0.7348584

Figure 1: The numerical solutions represent oscillating instanton solutions between flat-flat degenerate vacua.

The first figure illustrates the potential, where the number n denotes the number of the crossing. The maximum number $n_{max} = 6.$ The second figure illustrates the initial point Φo for each number of oscillation.

The figures (i), (iii), and (v) illustrate the tunneling starting from the left vacuum state to the right vacuum state. The figures (ii), (iv), and (vi) illustrate solutions going back to the starting point after oscillations. This type of solutions is possible only if gravity is taken into account.

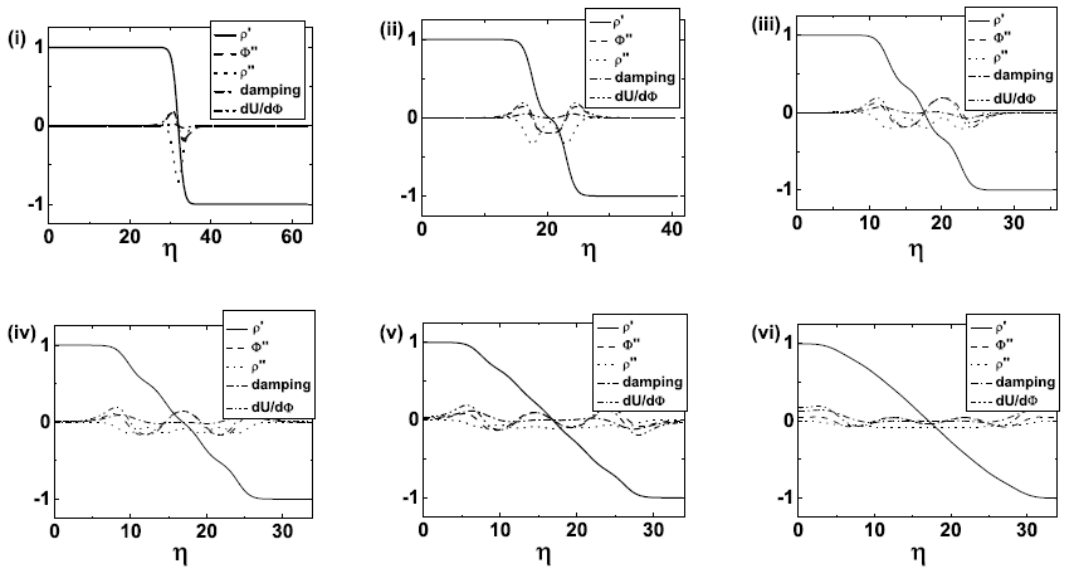

Figure 2: Variation of terms in equations of motion between flat-flat degenerate vacua.

Figure 2 shows the variation of terms, $\tilde{\rho}'$, $\tilde{\Phi}'$, $\tilde{\rho}''$, $\frac{3\tilde{\rho}'}{\tilde{\rho}}\tilde{\Phi}'$, and $d\tilde{U}/d\tilde{\Phi}$, with respect to $\tilde{\eta}$. The transition region of $\tilde{\rho}'$ means the rolling period in the inverted potential. In that region, every other terms also have dynamical behavior. All of behaviors represented in each figure can be understood with Z_2 symmetry.

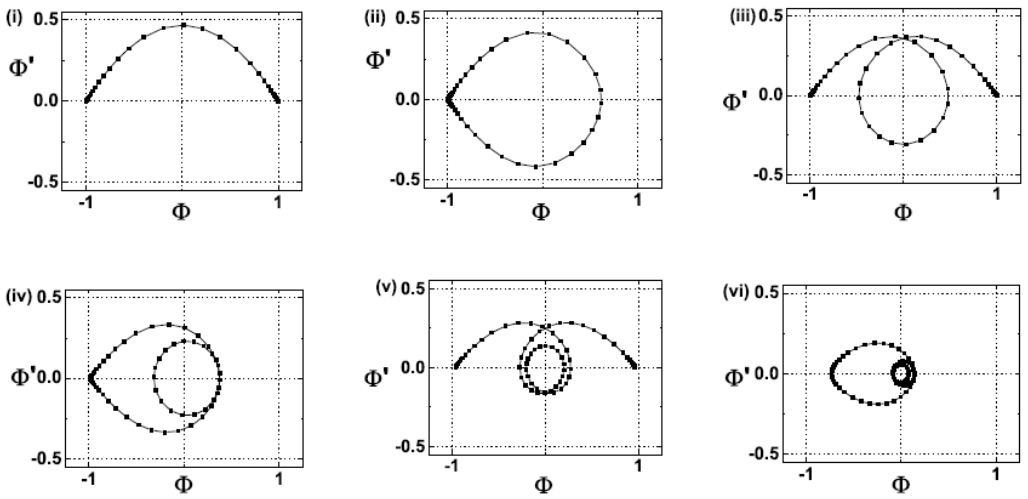

Figure 3: The behavior of the solutions in the Φ-Φ′ plane used the phase diagram method. The case is belong to the tunneling between flat-flat degenerate vacua.

The behavior of the solutions in the $\tilde{\Phi}(\tilde{\eta})$-$\tilde{\Phi}'(\tilde{\eta})$ plane used the phase diagram method is shown in Fig. 3. The figures (i), (iii), and (v) have the y-axis symmetry. The figures (ii), (iv), and (vi) have the x-axis symmetry. The maximum value of $\tilde{\Phi}'$ is decreased as the number of crossing is increased.

energy density $\xi \equiv -\mathcal{H} = -\left[-\frac{R}{2\kappa} + \frac{1}{2}\Phi'^2 + U\right] = U$

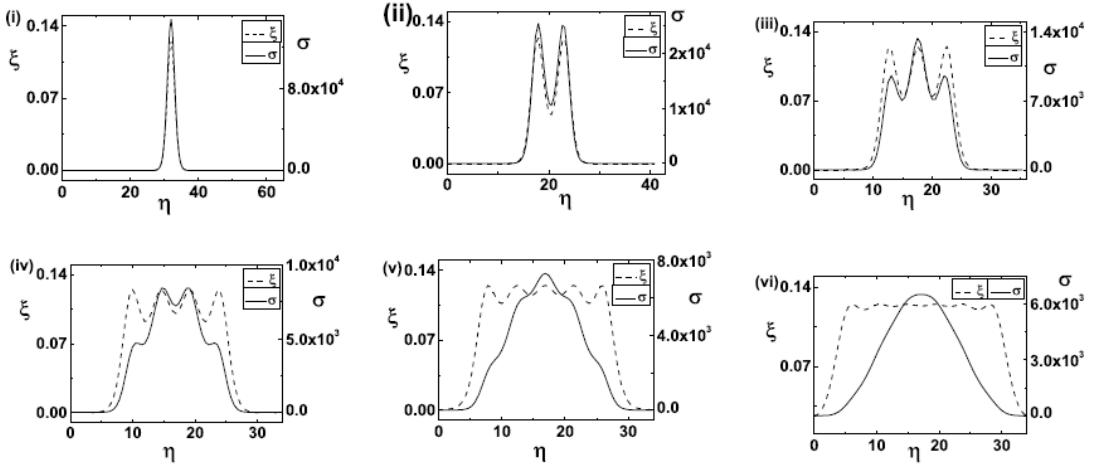

Figure 4: The diagram of energy density of each solutions. In each figure, the solid line denotes the surface energy density σ and the dotted line denotes the volume energy density ξ.

Figure 4 shows the diagram of the energy density of each solutions. The peaks represent the rolling phase in the valley of the inverted potential. The maximum value ξ_{max} is equivalent to U_{top}. The number of peaks is equal to the number of crossing. The peaks are broaden in range near U_{top} as the number of crossing increases. The surface energy density has also peaks. However, the shape of peaks becomes smooth and broadens as the number of crossing increases. As can be seen from the figure (vi), the thickness of the wall increases as the number of oscillations increases.

2.Oscillaing solutions between dS-dS degenerate vacua

($\tilde{U}_o = 0.5$ and $\tilde{\kappa} = 0.04$)

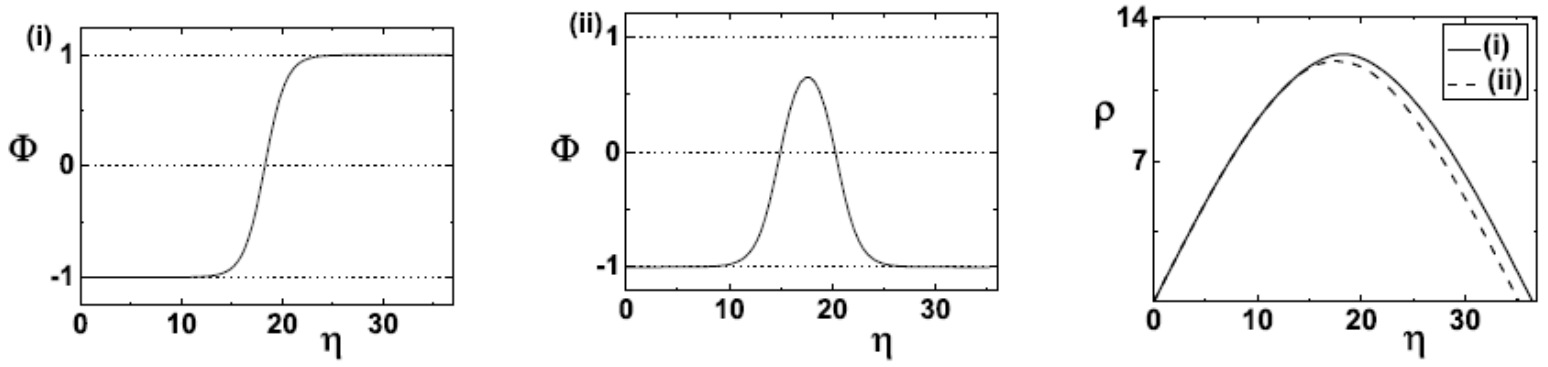

Figure 5: The numerical solutions between dS-dS degenerate vacua.

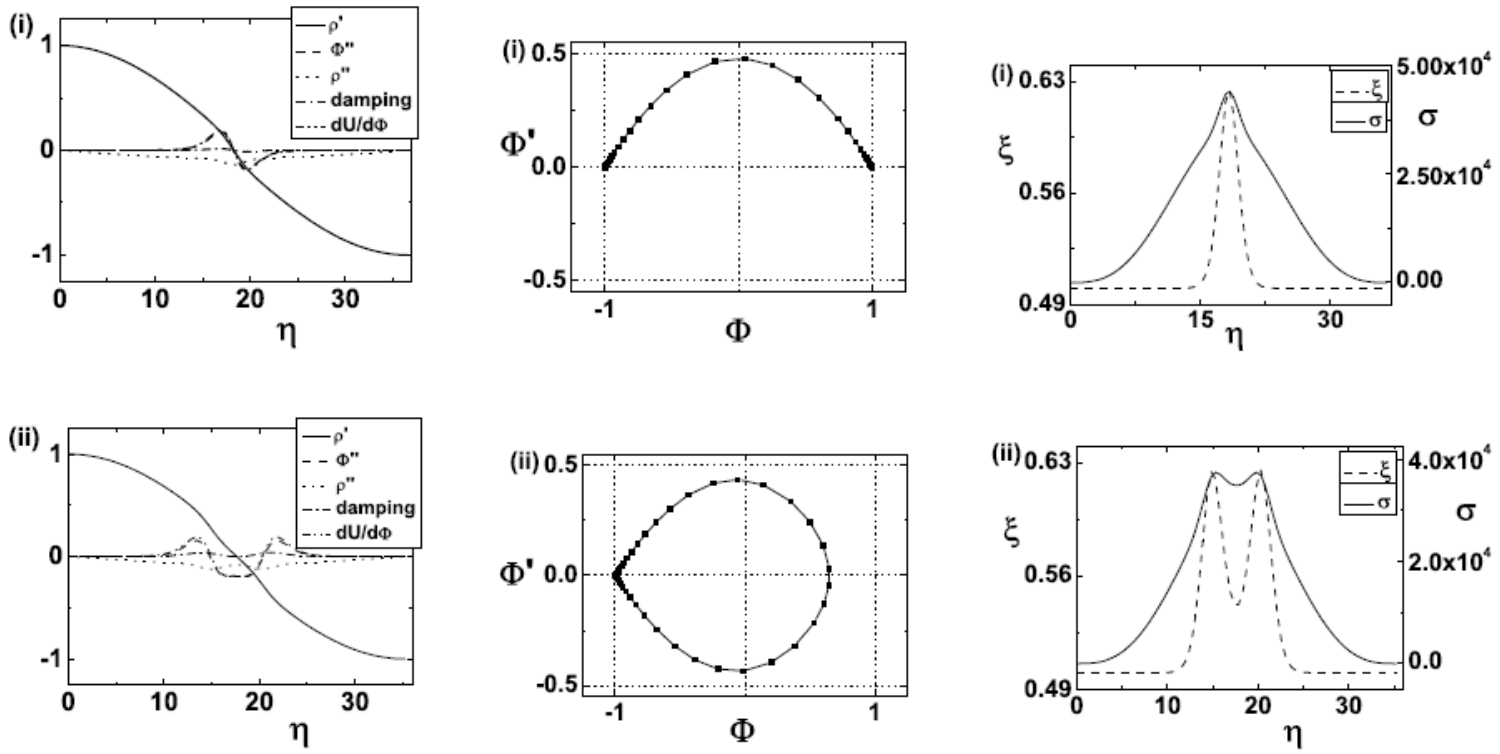

Figure 6: Variation of terms in equations of motion, phase diagrams, and the diagram of energy density between dS-dS degenerate vacua.

3.Oscillaing solutions between AdS-AdS degenerate vacua

($\tilde{U}_o = -0.02$ and $\tilde{\kappa} = 0.4$)

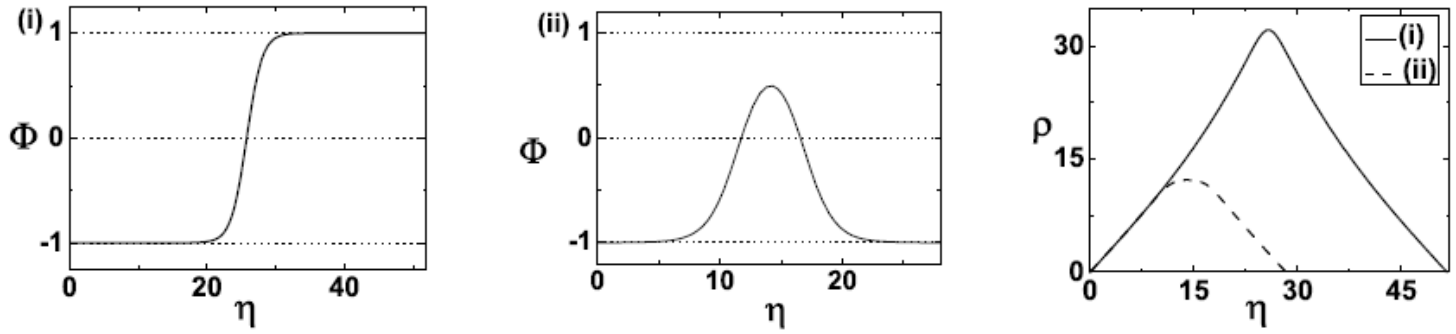

Figure 7: The numerical solutions between AdS-AdS degenerate vacua.

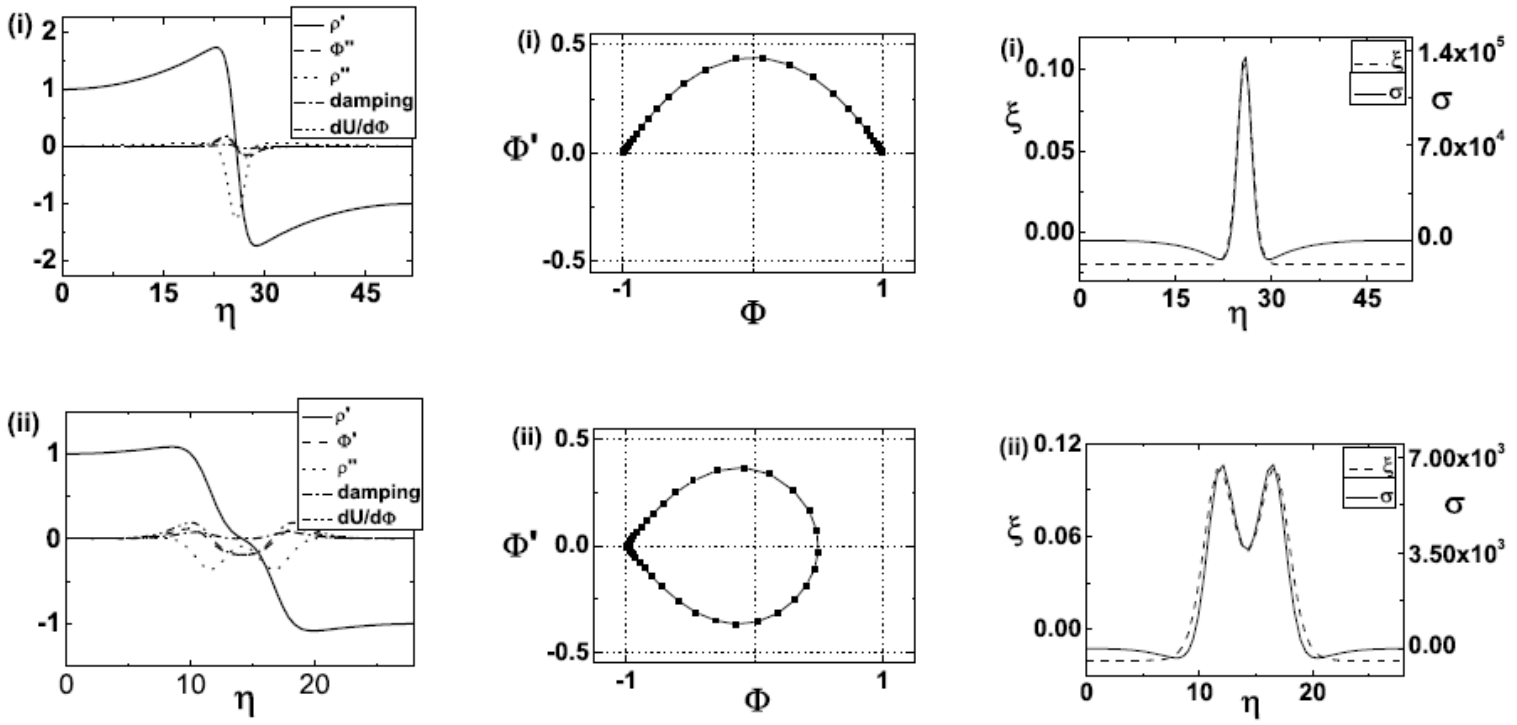

Figure 8: Variation of terms in equations of motion, phase diagrams, and the diagram of energy density between AdS-AdS degenerate vacua.

7. Nucleation of false vacuum bubbles

Bum-Hoon Lee, Chul H. Lee, WL and Changheon Oh, IJMPA30, 1550110 (2015)

From Zero to Eternity

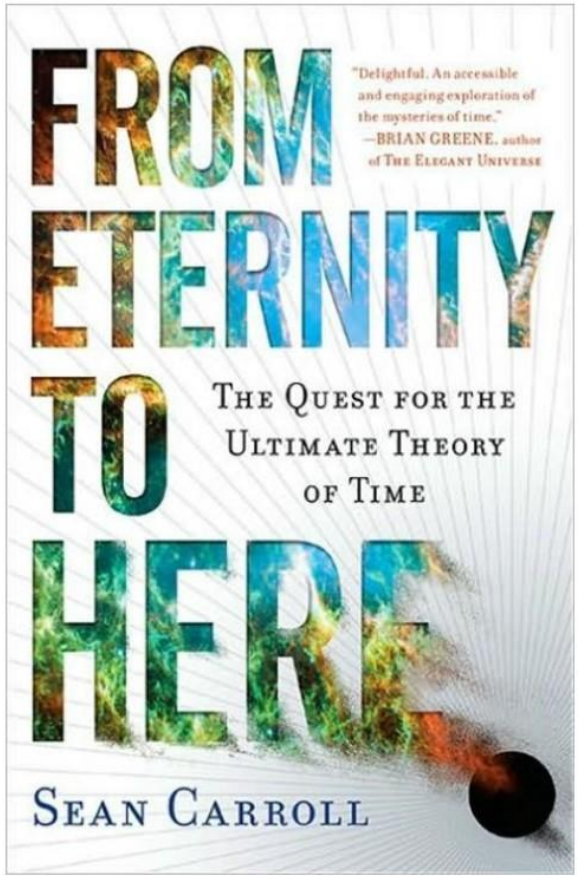

Schematic diagrams

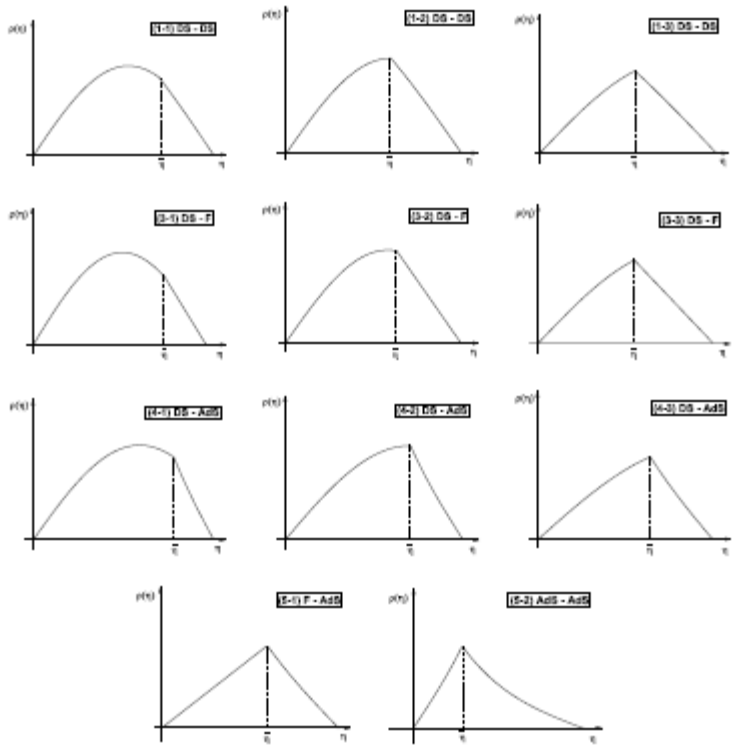

Figure 1-A

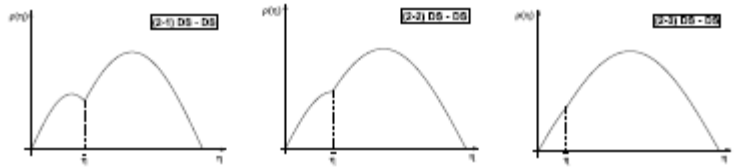

Figure 1-B

Figure 1: The schematic diagram for 14 possible types of false vacuum bubbles within finite true vacuum background or matching with the thin-wall approximation.

Numerical solutions : dS - dS

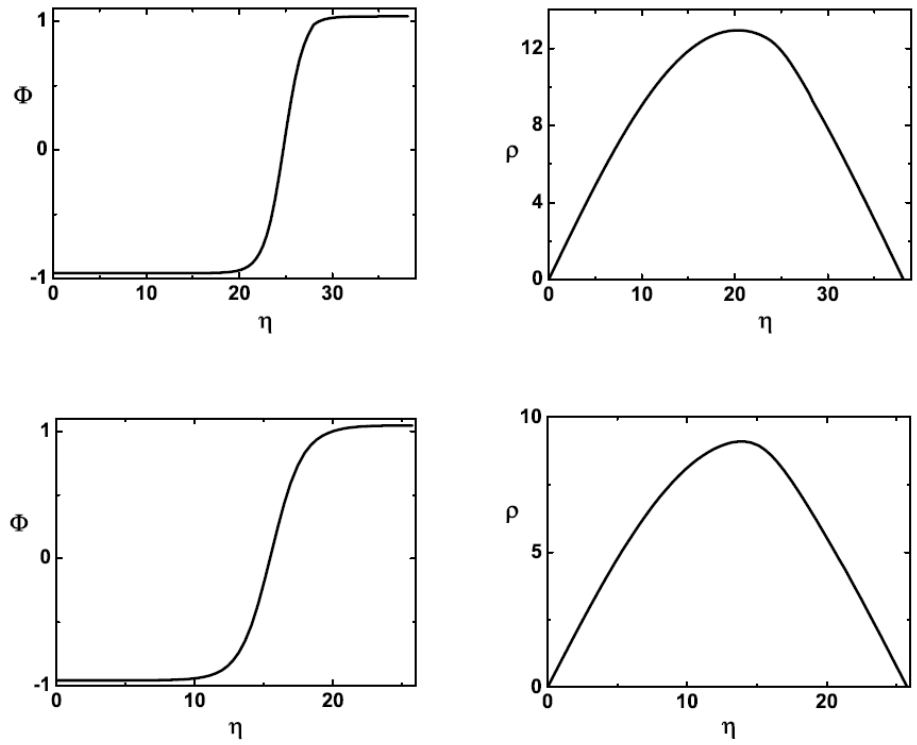

Figure 2: dS-dS cases. $\epsilon = 0.04$, $\kappa = 0.1$, and $U_0 = 0.1$ for for top figure. $\epsilon = 0.04$, $\kappa = 0.2$, and $U_0 = 0.1$ for for bottom figure.

dS-AdS

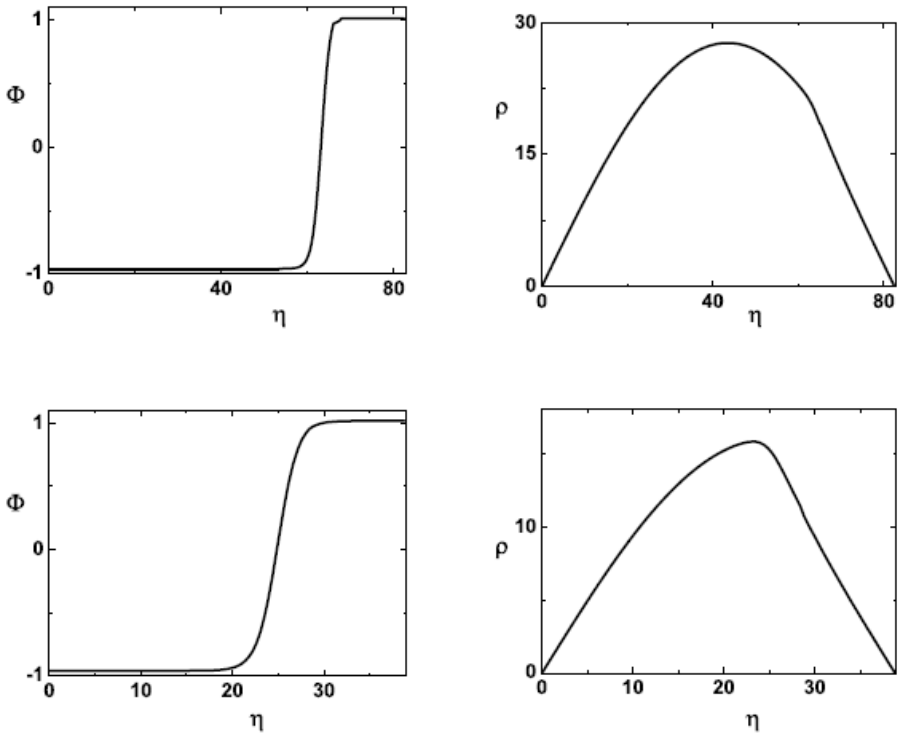

Figure 3: dS-AdS cases. $\epsilon = 0.04$, $\kappa = 0.1$, and $U_0 = -0.04$ for for top figure. $\epsilon = 0.04$, $\kappa = 0.3$, and $U_0 = -0.04$ for for bottom figure.

dS-flat

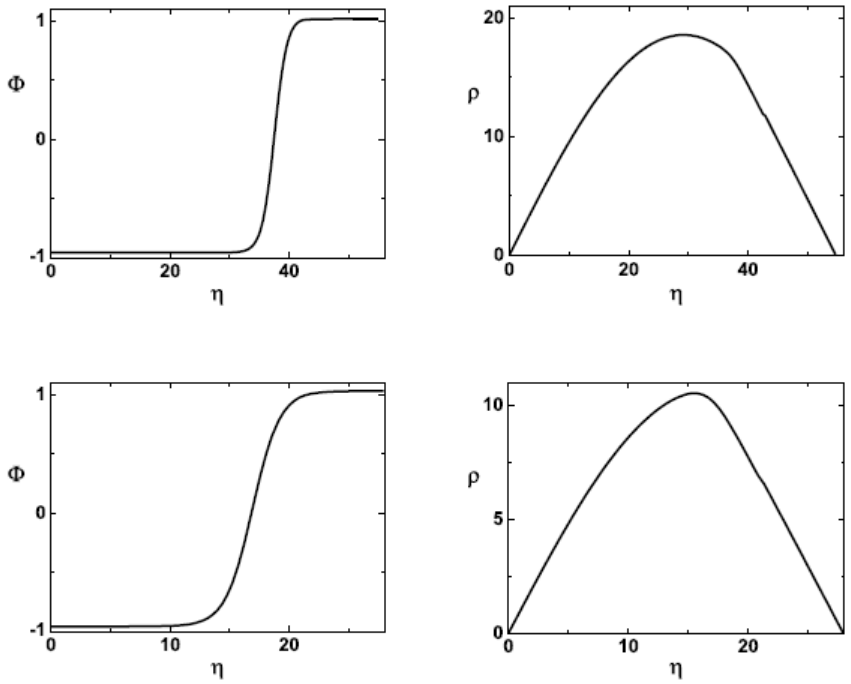

Figure 4: ds-flat cases. $\epsilon = 0.04$, $\kappa = 0.1$, and $U_0 = 0.0077$ for for top figure. $\epsilon = 0.04$, $\kappa = 0.3$, and $U_0 = 0.0077$ for for bottom figure.

flat-AdS and AdS-AdS

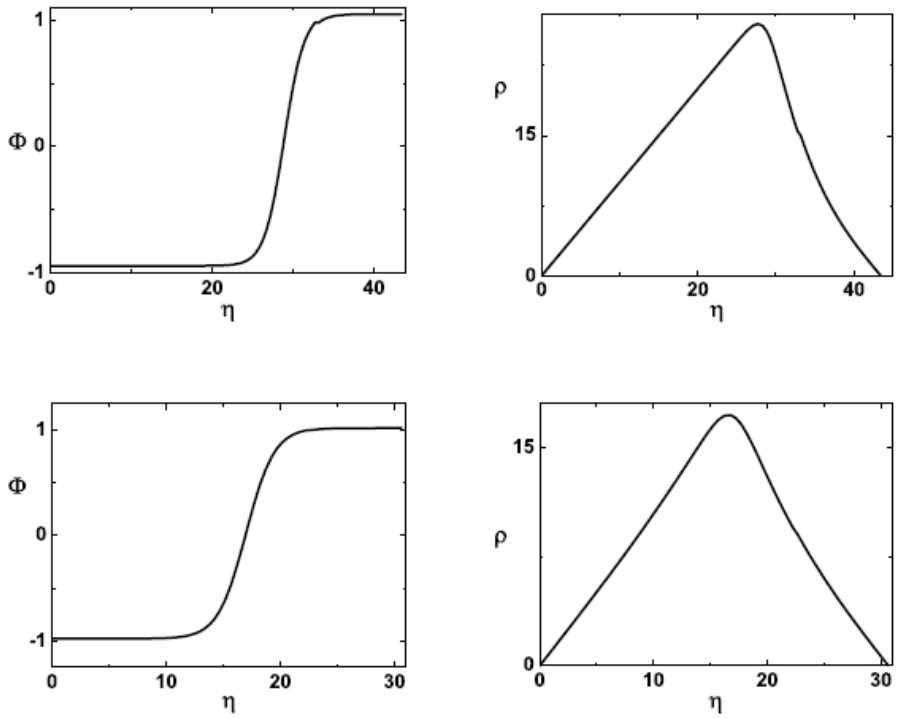

Figure 5: Flat-AdS and AdS-AdS cases. $\epsilon = 0.05$, $\kappa = 0.7$, and $U_0 = -0.09868$ for flat-AdS case. $\epsilon = 0.02$, $\kappa = 0.7$, and $U_0 = -0.05$ for AdS-AdS case.

Nucleation rate of a false vacuum bubble

We evaluate the nucleation rate

$$B = B_{in} + B_{wall} + B_{out}$$

The exponent B is the difference between the action of the bubble solution and that of the background geometry.

The Euclidean action is

$$S_E = \int_{\mathcal{M}} \sqrt{g_E} d^4x \left[-\frac{R}{2\kappa} + \frac{1}{2}\nabla^\alpha \Phi \nabla_\alpha \Phi + U(\Phi) \right] - \oint_{\partial\mathcal{M}} \sqrt{h_E} d^3x \frac{K - K_o}{\kappa}$$

For O(4)-symmetric solution,

$$S_E = 4\pi^2 \int_0^{\eta_{max}} d\eta \left[\rho^3 U - \frac{3\rho}{\kappa} \right] + \frac{6\pi^2}{\kappa}(\rho^2 \rho')|_{\eta_{max}} - \frac{2\pi^2 \rho^3}{\kappa}(K - K_o)|_{\eta_{max}}$$

where $K = \frac{3\rho'}{\rho}|_{\eta_{max}}$ and $K_o = \frac{3}{\eta}|_{\eta_{max}}$

The contribution of the wall

$$B_{wall} = 2\pi^2 \bar{\rho}^3 S_o$$

where the surface density or the tension of the wall $S_o (= \frac{2\mu^3}{3\lambda})$

The contribution from the inside part

$$B_{in} = \frac{12\pi^2}{\kappa^2}\left[\frac{-1 \pm (1-\frac{\kappa}{3}\bar{\rho}^2 U_F)^{3/2}}{U_F} - \frac{-1 \pm (1-\frac{\kappa}{3}\bar{\rho}^2 U_T)^{3/2}}{U_T}\right]$$

(1) (2)

(1) : + for the small bubble , - for the large dS bubble

(2) : + for the flat or AdS background, - for the dS background

The contribution from the outie part

$$B_{out} = \frac{12\pi^2}{\kappa^2 U_T}\left[2\left(1-\frac{\kappa}{3}\bar{\rho}^2 U_T\right)^{3/2}\right] + B_{feff}$$

where

$$B_{feff} = -\frac{12\pi^2}{\kappa^2 U_T}\left[1+\left(1-\frac{\kappa}{3}\tilde{\rho}^{i2}_{max} U_T\right)^{3/2}\right] - \frac{2\pi^2\rho^3}{\kappa} K_o|_{\eta_{max}}$$

The nucleation rate is

$$B = \frac{12\pi^2}{\kappa^2}\left[\frac{-1 \pm (1-\frac{\kappa}{3}\bar{\rho}^2 U_F)^{3/2}}{U_F} - \frac{-1-(1-\frac{\kappa}{3}\bar{\rho}^2 U_T)^{3/2}}{U_T}\right] + 2\pi^2\bar{\rho}^3 S_o + B_{feff}$$

The size of the bubble is determined by extremizing B.
The general formula

$$\bar{\rho}^2 = \frac{\bar{\rho}_o^2}{D}$$

where $\bar{\rho}_o = 3S_o/\epsilon$ **,** $D = \left[1 + 2(\frac{\bar{\rho}_o}{2\lambda_1})^2 + (\frac{\bar{\rho}_o}{2\lambda_2})^4\right]$, $\lambda_1^2 = [3/\kappa(U_F + U_T)]$, and $\lambda_2^2 = [3/\kappa(U_F - U_T)]$

After plugging the radius into the formula of the nucleation rate

$$B = \frac{2B_o[\{1 + (\frac{\bar{\rho}_o}{2\lambda_1})^2\} + D^{1/2}]}{[(\frac{\bar{\rho}_o}{2\lambda_2})^4\{(\frac{\lambda_2}{\lambda_1})^4 - 1\}D^{1/2}]} + B_{feff}$$

for dS B > 0, for flat B= $\frac{-24\pi^2(1+\frac{3\kappa S_o^2}{2\epsilon})}{\kappa^2\epsilon[1+(\frac{\bar{\rho}_o}{2\lambda_2})^2]^2}$ **and** $\frac{-24\pi^2}{\kappa^3 S_o^2}$ **.**

for AdS $B_{out} \to +\infty$ **i.e.** $B \to +\infty$.

The probability for the nucleation is exponentially suppressed.

8. Summary and discussions

In this work we classified the possible types of vacuum bubbles.

We expect that if the inverse tunneling from the flat or AdS to dS was possible in the very early universe the whole universe could be complete in the past direction without the initial singularity and the universe could be created from something within the multiverse or the cosmic landscape scenario. For the entropy issue, the scenario by the nucleation of a false vacuum bubble could also provide the beginning with a zero or very low entropy state.

The concept of the terminal vacuum or sink in the cosmic landscape scenario could be modified due to the nucleation of false vacuum bubbles.

There are unclear things: Geometry and probability

The detection of the gravitational wave over the CMBR could be open the door.

Thank you for your attention!